



## Full Length Article

# Biomechanics of horizontal meniscus tear and healing during knee flexion: Finite element analysis



Bingtong Yan<sup>a,b</sup>, Minmin Lin<sup>a,b</sup>, Yang Liu<sup>a,b</sup>, Jiawei Li<sup>a,b</sup>, Linjing Peng<sup>c</sup>, Yifei Yao<sup>c</sup>, Guangheng Li<sup>d,\*</sup>, Chao Liu<sup>a,b,\*\*</sup>

<sup>a</sup> Department of Biomedical Engineering, Southern University of Science and Technology, Nanshan District, Shenzhen, 518055, PR China

<sup>b</sup> Guangdong Provincial Key Laboratory of Advanced Biomaterials, Southern University of Science and Technology, Shenzhen, 518055, PR China

<sup>c</sup> Med-X Research Institute, School of Biomedical Engineering, Shanghai Jiao Tong University, 1954 Huashan Road, Xuhui District, Shanghai, China

<sup>d</sup> Division of Adult Joint Reconstruction and Sports Medicine, Department of Orthopedic Surgery, Shenzhen Key Laboratory of Musculoskeletal Tissue Reconstruction and Function Restoration, Shenzhen People's Hospital (the First Affiliated Hospital, Southern University of Science and Technology, The Second Clinical Medical College, Jinan University), Shenzhen, China

## ARTICLE INFO

## Keywords:

Biomechanics  
Finite element analysis  
Meniscus horizontal tear  
Knee joint

## ABSTRACT

Meniscus horizontal tear is a common injury that mostly occurs in middle-aged and elderly people, and the effect of repair surgery directly affects the functional recovery of the knee joint and prevention of degenerative joint diseases. However, the stress concentration in a horizontal tear is not well understood. The primary objective of this study was to examine the reparative mechanisms involved in addressing horizontal tears of the meniscus and to elucidate the alterations in mechanical behavior throughout the subsequent postoperative healing stages. Based on clinical MRI scan data of normal human knee joint, an accurate three-dimensional finite element model of the knee joint was established to simulate the meniscus at different states: including complete, horizontal torn, repaired and at different degrees of healing. An animal model was established to conduct in vitro loading experiments to assist in validating the model. Static standing simulation revealed the phenomenon of stress concentration in the area of horizontal tears. Knee flexion simulations identified the risk of tear propagation at the endpoints of the horizontal tear. Following suture repair and progressive healing, stress concentration was observed at the site of sutures, while the stress levels decreased at the endpoints of the horizontal tear. As healing progressed, the mechanical function of the meniscus gradually recovered. During progressive healing, the changing trends can provide a reference for patients' postoperative recovery activities. This finding has important implications for guiding clinical treatment strategies and rehabilitation plans for meniscal tears.

## 1. Introduction

The knee joint, as one of the most intricate and vital structures in the human body, plays a critical role in facilitating movement and bearing weight.<sup>1</sup> Central to the knee's function is the meniscus, a fibrocartilaginous structure that aids in load distribution, shock absorption, and joint stabilization.<sup>2,3</sup> In humans, menisci transmit 30–55 % of the load in a standing position and 90 % during knee flexion.<sup>1</sup> However, the complex biomechanical properties of meniscus also make them susceptible to a variety of injuries, among which meniscal tears are particularly common.<sup>4</sup>

Meniscal injuries present a significant challenge in orthopedic and sports medicine due to their impact on the knee's functionality and the quality of life.<sup>5</sup> Meniscus tears are a recognized risk factor for the onset of posttraumatic osteoarthritis (OA), contributing to approximately 12 % of all cases of knee OA.<sup>6</sup> Between 6 and 20 years after sustaining meniscal tears, approximately 50 % of individuals show radiographic signs of OA.<sup>7,8</sup> One of the common types of meniscal tears is the horizontal tear, which divides the meniscus into two layers, the superior and inferior leaflets.<sup>9</sup> Meniscus horizontal tears are mostly degenerative and often occur in the posterior horn of the medial meniscus, with suturing being

This article is part of a special issue entitled: Bone Mechanobiology published in Mechanobiology in Medicine.

\* Corresponding author.

\*\* Corresponding author. Department of Biomedical Engineering, Southern University of Science and Technology, Nanshan District, Shenzhen, 518055, PR China.

E-mail addresses: [12232615@mail.sustech.edu.cn](mailto:12232615@mail.sustech.edu.cn) (B. Yan), [11712435@mail.sustech.edu.cn](mailto:11712435@mail.sustech.edu.cn) (M. Lin), [12131143@mail.sustech.edu.cn](mailto:12131143@mail.sustech.edu.cn) (Y. Liu), [12232622@mail.sustech.edu.cn](mailto:12232622@mail.sustech.edu.cn) (J. Li), [penglinjing1995@sjtu.edu.cn](mailto:penglinjing1995@sjtu.edu.cn) (L. Peng), [yifeiyao@sjtu.edu.cn](mailto:yifeiyao@sjtu.edu.cn) (Y. Yao), [liguangheng@hotmail.com](mailto:liguangheng@hotmail.com) (G. Li), [liuc33@sustech.edu.cn](mailto:liuc33@sustech.edu.cn) (C. Liu).

<https://doi.org/10.1016/j.mbm.2025.100128>

Received 21 November 2024; Received in revised form 24 February 2025; Accepted 7 March 2025

Available online 13 March 2025

2949-9070/© 2025 The Author(s). Published by Elsevier B.V. on behalf of Shanghai Ninth People's Hospital, Shanghai Jiao Tong University School of Medicine. This is an open access article under the CC BY-NC-ND license (<http://creativecommons.org/licenses/by-nc-nd/4.0/>).

the common treatment method.<sup>10</sup> Due to the degenerative process of meniscus horizontal tears, the risk of developing symptoms increases as the tears extend.<sup>11</sup> Unlike other traumatic tears, horizontal tears involve more complex mechanical changes due to the better preservation of circumferential fibers.<sup>12</sup> Such prognostic evaluations are vital for informing patients of their recovery outlook and guiding therapeutic decisions.<sup>13–15</sup>

The meniscus contains a unique blood vessel network that influences its healing potential. The peripheral regions, known as the red-red zone, has abundant vascularization; while the red-white zone has limited blood supply, and the white-white zone is avascular.<sup>16</sup> This vascular distribution affects the repair outcomes of meniscal tears, especially those located in the less vascularized areas. The peripheral 10%–30 % of the meniscus is vascularized, allowing for better healing potential. The red-white zone, which is partially vascularized, shows a healing rate of approximately 83 % for repairs.<sup>17</sup> The white-white zone is typically considered irreparable due to its lack of blood supply. Horizontal tears, particularly those spanning all zones, have poor repair outcomes and are degenerative.

In the realm of biomechanics, finite element analysis (FEA) has emerged as a powerful tool.<sup>18–20</sup> However, the limitations of current researches predominantly involve applying static axial load.<sup>21–23</sup> Under static standing conditions, the influence of meniscus injury on knee joint mechanics is limited, making it less relevant to daily activities.

The biomechanical response of meniscus exhibits a strong dependence on knee joint angle.<sup>24</sup> It was observed that the posterior horn of the meniscus bore the highest proportion of shear load, particularly when a posterior shear force was applied after reaching 30 degrees of flexion. In this scenario, the meniscus was estimated to bear approximately 50 % of the shear force.<sup>25</sup> However, the variations in stress distribution of the meniscus at different knee joint angles are not yet well understood.

The purpose of this study was to explore the biomechanics of meniscus during knee flexion. This research investigated the biomechanical effects of horizontal tear and healing at the posterior horn of the medial meniscus.<sup>25</sup> To our knowledge, this is the first study fitting the correlation between progressive healing after horizontal tear repair and the mechanical responses of the meniscus, thereby providing a theoretical foundation for the diagnosis and treatment of meniscal horizontal tears.

## 2. Materials and methods

### 2.1. Data acquisition and three-dimensional reconstruction of the knee joint

Magnetic resonance imaging (MRI) generates high resolution image of soft-tissue. The left knee joint of a 26-year-old healthy male volunteer was selected for MRI, with a thickness of 0.45 mm between slices. A total of 423 MRI images were obtained. The DI-COM-format images of the knee joint were segmented to generate three-dimensional model in Mimics 21.0 software (Materialise, Leuven, Belgium).

The procedure for obtaining human tissue samples from hospitals was approved by the medical ethics committee of Shenzhen People's Hospital (approval number: LL-KY-2023061; Title: Investigation of biomechanics of horizontal meniscus tear and progressive healing; Date of approval: 01/04/2023).

To minimize variation in the models, manual segmentation was performed under the guidance of an orthopedic surgeon. Thresholding was used to select appropriate region to create masks for segmentation. Given that real images often contain noise and artifacts, the initial masks require optimization. Masks were refined, enhancing reconstruction accuracy. Finally, 3D calculations were performed to reconstruct masks into solid objects, building a knee joint model that reflects its anatomical features, including models of the femur, tibia, articular cartilage and menisci.

To optimize the grid density for ensuring calculation accuracy, the FE model was remeshed with uniform surface and directly converted into optimized tetrahedral elements. The three-dimensional model of the knee joint was optimized in 3-matic software (Materialise, Leuven, Belgium).

### 2.2. FE modelling and material properties

In Abaqus 6.19 software (SIMULIA, Rhode Island, USA), material assignment, boundary conditions, interaction constraints and analysis steps were set to establish a complete three-dimensional finite element knee joint model (Fig. 1A). Based on the intact meniscus, models were established to simulate meniscus with horizontal tear, sutured repair, and progressive healing after repair surgery. The horizontal tear and sutured repair model were primarily compared to the intact model, while the progressive healing models served as another group of comparisons.

Based on the intact medial meniscus, to simplify the model for horizontal tear of the meniscus, a transverse wedge defect was used to simulate a grade III horizontal tear. Within the range of the posterior horn of the medial meniscus, a complete tear of the posterior root of the medial meniscus was simulated, terminating at the bony stop point of the tibial attachment. The length of the tear along the inner edge was 1.49 cm, and the length of the tear along the outer periphery was 1.46 cm.

In the sutured repair model, based on the horizontal tear model, sutured repair surgery were simulated with a sutured spacing of 0.4–0.6 cm. Considering the length of the tear along the inner edge, two stitches were selected, placed on both sides of the tear edge to ensure uniformity of the sutures and stability of tear closure.<sup>26,27</sup> This distribution helps to evenly distribute tension along the tear edge, reduce stress concentration at the tear site, and promote healing.

The progressive healing models were simulated considering the blood supply of the meniscus, and the healing range extended from the red zone to the white zone.<sup>28</sup> When a meniscal tear occurs in the red zone, it has stronger healing capability due to an adequate blood supply. Tears occurring in the red-white zone also have some healing capacity. Meniscal tears occurring in the white zone have poor healing ability due to limited blood supply.<sup>29</sup> The simulated progressive healing model of the horizontal meniscal tear includes the following five types, based on the red and white zones and the healing trend of the meniscus: 50 % healing in the red zone (R–R 50 %), 100 % healing in the red zone (R–R 100 %), 50 % healing in the red-white zone (R–W 50 %), 100 % healing in the red-white zone (R–W 100 %), and 50 % healing in the white zone (W–W 50 %). Each model's healing is established based on the previous healing model in order. Despite the clinical observation that healing in the white zone is difficult, healing models corresponding to the red and red-white zones are still set for the white zone to observe and compare their mechanical responses. The healing model is established based on the suture model, which limits the relative motion of the upper and lower leaflets of the meniscus while the tear along the inner edge of the meniscus is constrained by the simulated sutures.

The material properties of individual component were determined based on previously published data and were currently defined as isotropic linear elastic materials with the parameters shown in Table 1. The ligaments and attachments of meniscus horns were simulated by axial connectors (Fig. 1B and C).

In the FE model of knee joint, the meniscus was assigned an anisotropic material property using discrete orientation.<sup>30,31</sup> Discrete orientation allows the meniscus to be defined in the local material directions, and be modeled with different elastic moduli in the radial, circumferential, and axial directions. This can reflect the influence of collagen fibers on the mechanical behavior of the meniscus.<sup>32</sup>

### 2.3. Loads and boundary conditions

For the axial load, 50 % of the body weight is applied to the superior surface of the femur, and knee flexion is controlled by setting the rotation

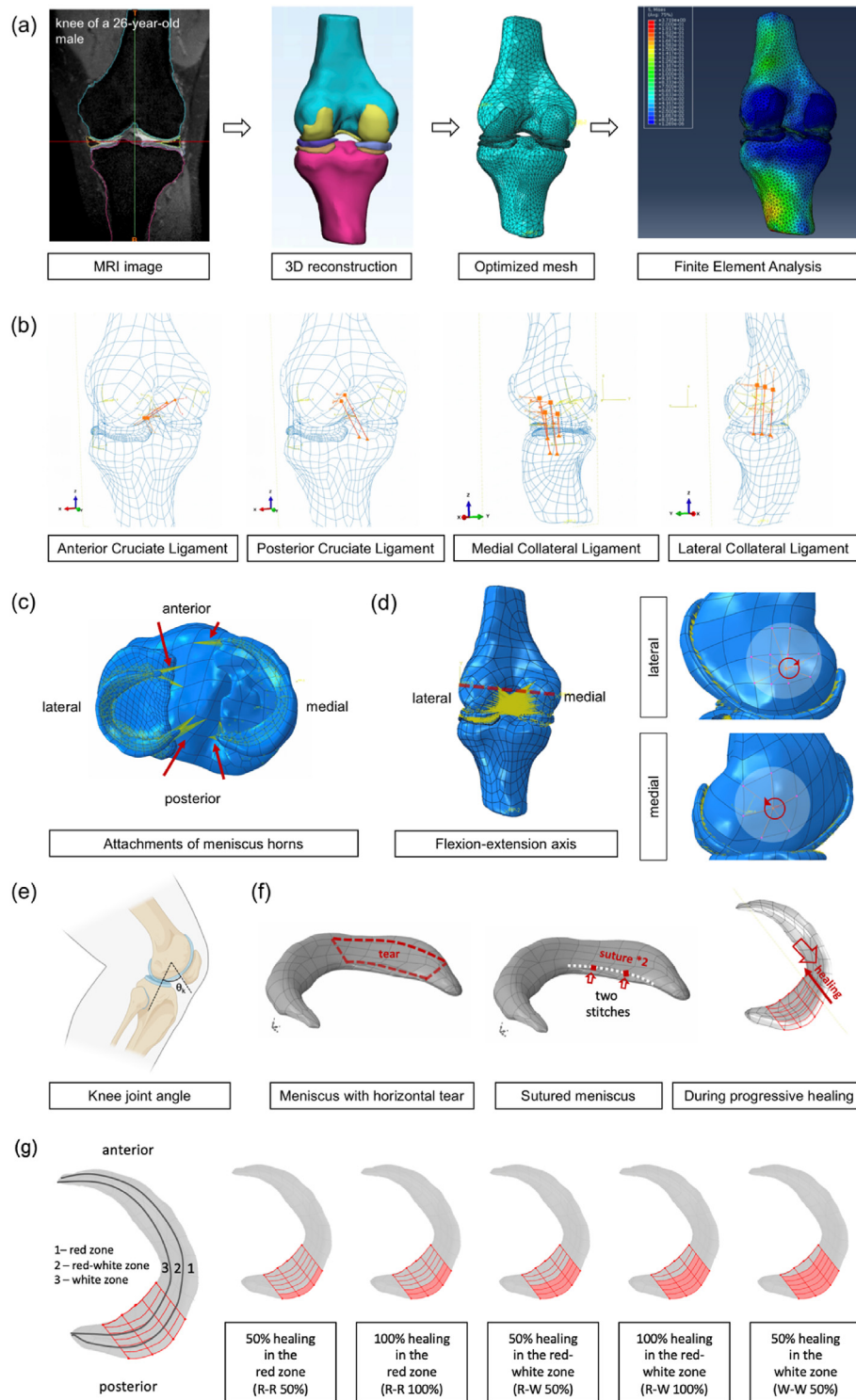


**Fig. 1.** 3D models used in the FE simulation (a) Study workflow, (b) the simulation of ligaments, (c) the simulation of attachments of meniscus horns, (d) the simulation of flexion–extension axis of knee joint, (e) knee joint angle ( $\theta_k$ ), (f) FE model of meniscus tear, suture repair and healing simulation, and (g) diagram of progressive healing models.

axis of the knee joint. For an example of a healthy 26-year-old male with a height of 180 cm and a weight of approximately 70 kg (which is within the normal Body Mass Index range of 18.5–24.9), the axial load corresponding to 50 % of body weight is approximately 343 N. In this study, the load conditions try to simulate the assisted knee flexion during the rehabilitation process after the tear repair, i.e. the knee joint bears the same perceived load at each angle.

The boundary conditions were defined as follows: the bottom end of the tibia was fully fixed in 6 degrees of freedom, and the femur was unconstrained for all translational and rotational degrees of freedom. The interaction module was loaded and 6 groups of contact surfaces were set: the medial compartment, including femoral cartilage - tibial cartilage, femoral cartilage - medial meniscus, and medial meniscus - tibial articular cartilage surfaces; and the lateral compartment, including femoral

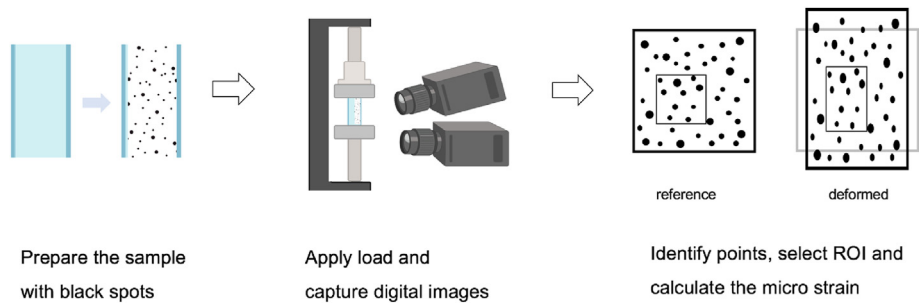


Fig. 2. Workflow of using digital image correlation to measure strain field.

Table 1  
Material properties assigned to FE model.

Component	Elastic modulus (MPa)	Poisson's ratio	Density (kg/m <sup>3</sup> )	Property	References
Bone	13000	0.3	2000	Rigid	39,40
Articular cartilage	15	0.46	1350	Isotropic	41,42
Meniscus	(Circumferential) 120 (Axial) 20 (Radial) 20	(Circumferential) 0.2 (Axial) 0.3 (Radial) 0.3	1100	Transversely isotropic	42–44

cartilage - tibial cartilage, lateral meniscus - femoral cartilage, and lateral meniscus - tibial cartilage surfaces. A joint interface was defined as a hard contact with  $\mu = 0.002$  friction coefficient, no penetration, and limited slip.<sup>33</sup>

The axis of rotation of the knee joint was defined as the line connecting the most prominent points of the medial and lateral condyles of the femur, which was also the line connecting the origins of the medial and lateral collateral ligaments (Fig. 1D). To simulate knee flexion and extension of the knee joint, the knee joint angle changes from 0° to 90° (Fig. 1E). A coupling constraint was applied to the endpoints of the axis of rotation and the surfaces of the medial and lateral condyles of the femur. Given that the femur was defined as a rigid body, this enabled the axis of rotation to drive the rotation of the femur.

For the horizontal tear model, the contact between the superior and inferior leaflets at the site of horizontal meniscal tear was defined as hard contact with a friction coefficient of 0.002 and penalty sliding surface-to-surface contact, as there was no direct constraint between them. For the sutured repair model, sutured repair was simulated by applying tie constraints between the two adjacent nodes along the vertical inner edge of the superior and inferior leaflets. The tie constraints were used to partially restrict the degrees of freedom between the nodes, aiming to approximate the actual sutured surgery. For the progressive healing models after surgery, the different degrees of healing in the torn

meniscus were simulated by constraining the relative motion between the superior and inferior leaflets (Fig. 1F). Specifically, this was achieved by coupling the lower surface of superior leaflet and the upper surface of inferior leaflet.

2.4. Digital image correlation

To identify the risk of tear propagation of horizontal tear, an ex vivo loading experiment was conducted on the rabbit knee joint to measure the strain distribution on the surface of the meniscus posterior horn. The upper and lower ends of the knee joint were fixed with bone cement to align femur and tibia to simulate upright posture in humans. A compressive force of 9 N was applied axially, based on the body weight of the rabbit used in our study, which was 3.7 kg. This load simulates the static condition of the rabbit standing on all fours while controlling for variables in comparing the mechanical responses before and after the horizontal tear. To observe the strain concentration at the surface of the meniscus, the femur, tibia (Fig. 3A), articular cartilage, and other ligaments except the medial collateral ligament were remained.

During the experiment, a series of digital images are captured using a high-speed camera. The initial image, representing the initial state, is compared with subsequent images taken during and after the application

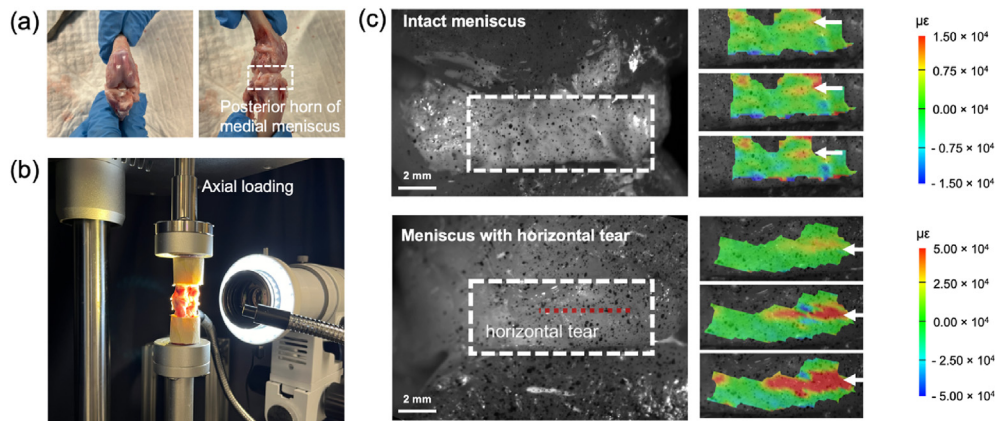


Fig. 3. Ex vivo loading experiment of rabbit knee joint to validate the FE model (a) Ex vivo model, (b) loading test with tensile testing machine, (c) micro strain field on meniscus surface measured by DIC; red dotted line, horizontal tear.



of the axial compressive force (Fig. 3B). Utilizing advanced image processing algorithms and correlation software, the displacement vectors and strain fields are calculated by correlating the speckle patterns in the reference image with those in the deformed images (Fig. 2).

### 3. Results

#### 3.1. Static standing simulation to validate FE model

Under the final loaded state, the strain value was significantly higher than the intact meniscus (Fig. 3C). According to the DIC results, the intact meniscus had a maximum strain of  $1.50 \times 10^4$  microstrain when loaded to 9 N, concentrated in the horizontal linear region of the outer surface, consistent with common locations of horizontal tears. The meniscus with horizontal tear had a maximum strain of  $5.00 \times 10^4$  microstrain when loaded to 6 N, with strain clearly manifesting along the tear.

The finite element analysis results align with clinical observation, of which clinical cases of meniscal tears commonly occur at the posterior horn of lateral meniscus and anterior horn of medial meniscus during static standing (Fig. 4). Due to the anisotropic nature of meniscus, the fatigue strength of the meniscus is not a well-defined value. Therefore, we employed a reference fatigue strength of 3 MPa, which is based on the fatigue strength of articular cartilage.<sup>34</sup>

#### 3.2. Horizontal tear and sutured repair simulation during knee flexion

The risk of tear propagation could be assessed by observing the stress distribution around the potential tear site of the meniscus tear (Fig. 5). During knee flexion and extension of the knee joint, from the knee joint angle of  $0^\circ$ – $90^\circ$ , as the flexion angle increases, the area of stress concentration on the medial meniscus moves from the posterior horn region towards the anterior horn region.

For the meniscus with horizontal tear, the stress level increases significantly in the tear region, with stress concentrations appearing on the peripheral undersurface around the tear and along the tear path on the inner edge. Peak stresses typically occur at the anterior and posterior endpoints of the tear, risking further tear propagation. For a repaired meniscus after sutured, sutured cannot fully restore the biomechanical response to the intact meniscus, but does reduce stresses in the peripheral tear region slightly. However, stress concentrations appear at the suture points near the inner edge region, reducing the risk of further tear propagation.

For meniscus horizontal tear, peak stresses typically occur at the peripheral endpoints of the tear, with higher peak stresses in the superior leaflet compared to the inferior leaflet (Fig. 6). There are obvious stress concentrations along the anterior and posterior tear edges. During knee flexion, since the inner tear edge contacts the articular cartilage over larger area than the periphery, there is significant stress concentration along the inner edge of the superior leaflet tear.

For a surgically repaired meniscus after sutured, peak stresses tend to occur at the suture points along the inner tear edge, especially near the posterior root attachment. In contrast to the horizontal tear, peak stresses are higher in the inferior leaflet compared to the superior leaflet. Similarly to the horizontal tear, stress concentrations are present along the anterior and posterior tear edges and surrounding areas. Compared to the

horizontal tear, stress levels are slightly reduced along the anterior and posterior tear edges in the repaired model.

#### 3.3. Healing simulation during knee flexion

After suture treatment, there was a noticeable concentration of stress at the suture site, appearing as discrete stress peaks. Due to the poor healing capacity of the white zone, there is a greater risk of propagation of tears in this area. Therefore, particular attention was given to the stress levels at the anterior and posterior endpoints of the tear (Fig. 7). During knee flexion, the stress distribution changes similarly in the progressive healing models of the meniscus. The peak stress at the endpoints decreases, but there are instances where it still exceeds 3 MPa, particularly when healing occurs solely in the red zone at the anterior endpoints. This suggests a certain risk of tear propagation exists, but overall, the risk of tear propagation at the endpoints is significantly decreases after repair.

For the tear region, there is a significant increase in stress levels, particularly in the range near the periphery (Fig. S1). With increasing knee flexion angle, the stress concentration area on the superior surface of the posterior horn spreads from the periphery towards the inner edge, while the stress concentration area on the inferior surface of the posterior horn moves towards the outer periphery. As the meniscus gradually slides relative to the tibial plateau, the stress concentration area moves towards the inner edge.

Observing the stress distribution on the inferior surface of the superior leaf during progressive healing (Fig. S2). The stress concentration region is located near the anterior and posterior endpoints of the tear.

### 4. Discussion

In this study, a finite element model of the human knee joint with horizontal tear meniscus was established, and in conjunction with current clinical treatment, surgical sutured repair and postoperative progressive healing models of the meniscus in the human knee joint were developed. This research filled the gap in numerical simulation studies related to meniscus horizontal tear and simulated the progressive healing process after surgical repair. For the first time, the mechanical response changes of meniscus horizontal tear and the sutured repair during knee flexion were analyzed. The results might provide guidance for the evaluation and treatment of horizontal meniscus tears. An animal model in the knee joint was loaded to validate the FE model, and digital image correlation was used to observe the micro strain of the meniscus. The experimental results revealed the phenomenon of stress concentration in the horizontal tear region and were compared with the simulation results.

Current biomechanical studies on meniscus using finite element analysis primarily focuses on specific types of meniscus injuries. The established knee joint FE models generally encompass comprehensive analyses involving meniscal tears, meniscectomy, meniscal implants, and intact meniscus. However, biomechanical studies on meniscal tears mainly concentrate on radial tears and traumatic tears, with limited research on horizontal tears.<sup>35</sup> The stress distribution caused by horizontal tears in the meniscus remains unclear. It has been suggested that horizontal tears in the meniscus are often associated with long-term joint wear and degeneration. Under abnormal knee joint postures, the stress

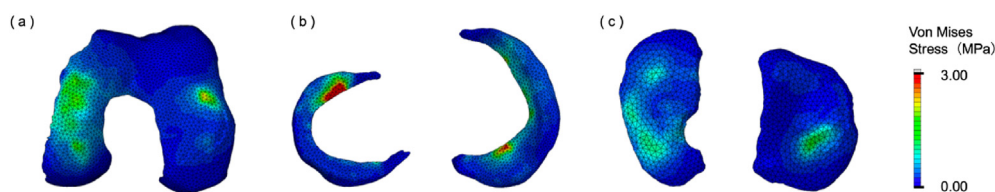


Fig. 4. Stress distribution of soft tissues (a) femoral articular cartilage, (b) menisci, and (c) tibial articular cartilage during static standing simulation, with 50 % of the body weight applied axially to the femur.

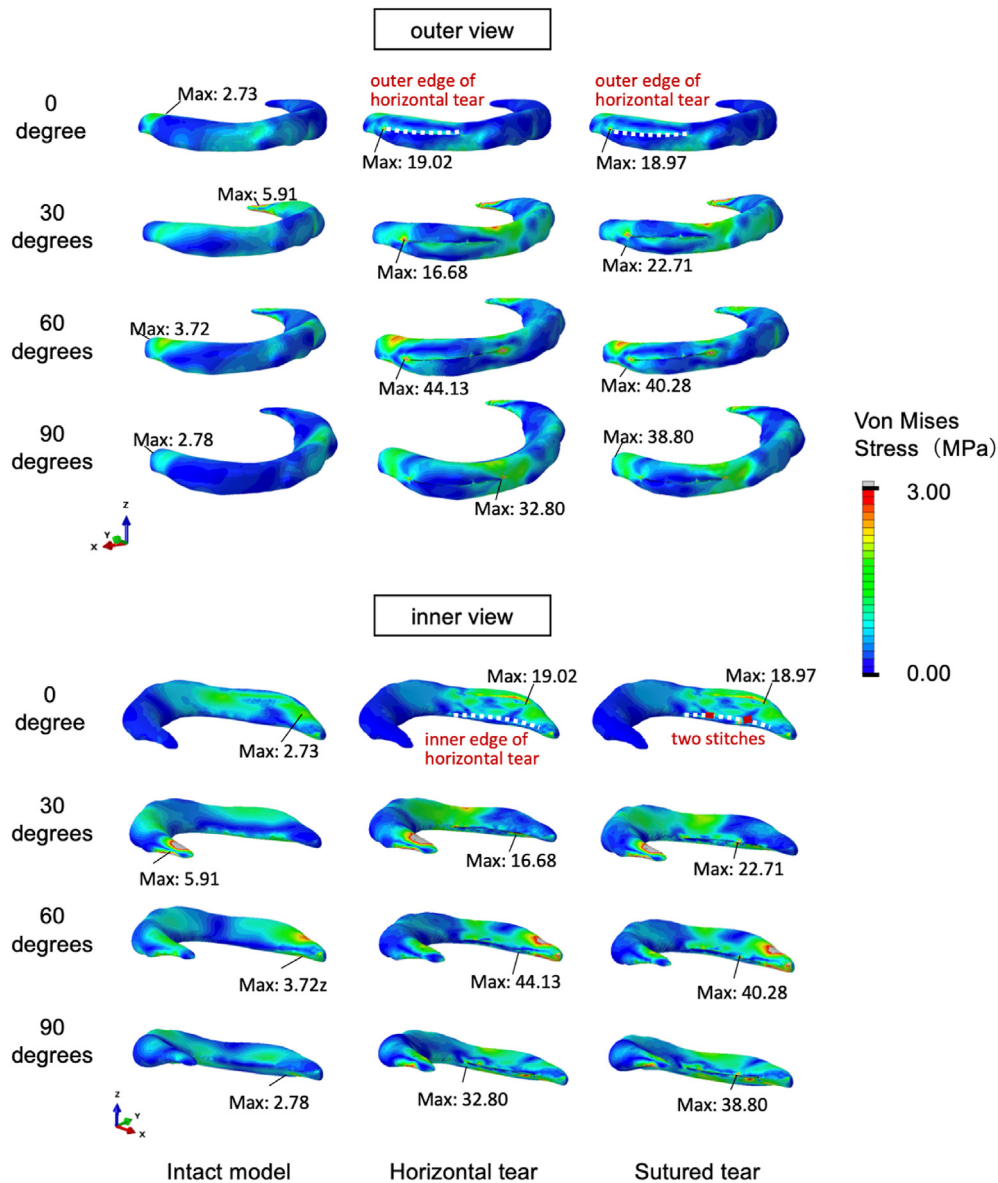


Fig. 5. Stress distribution around the potential tear site with the knee flexion angle of 0 degree, 30 degree, 60 degree and 90 degree.

distribution on the meniscus becomes uneven, thereby increasing the risk of tears.<sup>36,37</sup> Investigating the biomechanical characteristics of the knee joint under different postures contributes to a better understanding of stress concentration and other biomechanical mechanisms involved in horizontal meniscal tears, guiding clinical treatments and rehabilitation strategies. This study explored the biomechanical changes using an optimized finite element model of human knee joint, under meniscus horizontal tear and progressive healing simulation after sutured repair surgery. The FE model was validated by *ex vivo* loading experiment of rabbit knee joint, and the mechanical effects of horizontal tear, suture repair, and progressive healing on the meniscus were analyzed using finite element analysis during knee flexion. The horizontal tear and sutured repair models were primarily compared to the intact model, while the progressive healing model served as another comparison group.

Most of the current biomechanical studies related to the meniscus simulate the knee joint in a static upright position. The established finite element models of the knee joint typically include the femur, articular cartilage, medial and lateral menisci, and tibia, with a few models incorporating solid ligament constraints. Despite existing research on the biomechanics of meniscal tears in the knee joint, the analysis has mainly

focused on static standing conditions, while the understanding of horizontal meniscal tears during knee flexion remains limited. Under static standing conditions, the influence of healthy menisci on knee joint mechanics is limited and has low relevance to daily activities. Furthermore, most studies, whether involving meniscal implants or simulating intact autologous menisci, assume that the meniscus is isotropic and uniform, which does not align with the actual mechanical characteristics of the meniscus. In this study, the meniscus was assigned an anisotropic material property using discrete orientation, which could reflect the influence of collagen fibers on the mechanical behavior of the meniscus.

This study established a model of horizontal meniscal tear injury in the human knee joint and further developed models for surgical repair of horizontal meniscal tears and postoperative progressive healing, incorporating current clinical treatment approaches. The primary factor in reducing the risk of tear propagation is the suturing repair. During the healing process, the differences in healing stages may not be as significant as initially implied. However, for the FE model, the effects of ligaments were simplified and the effects of muscle were ignored, the viscoelastic characteristics of soft tissues would be closer to reality if they were under nonlinear simulation.<sup>38</sup> In future, this study can be extended

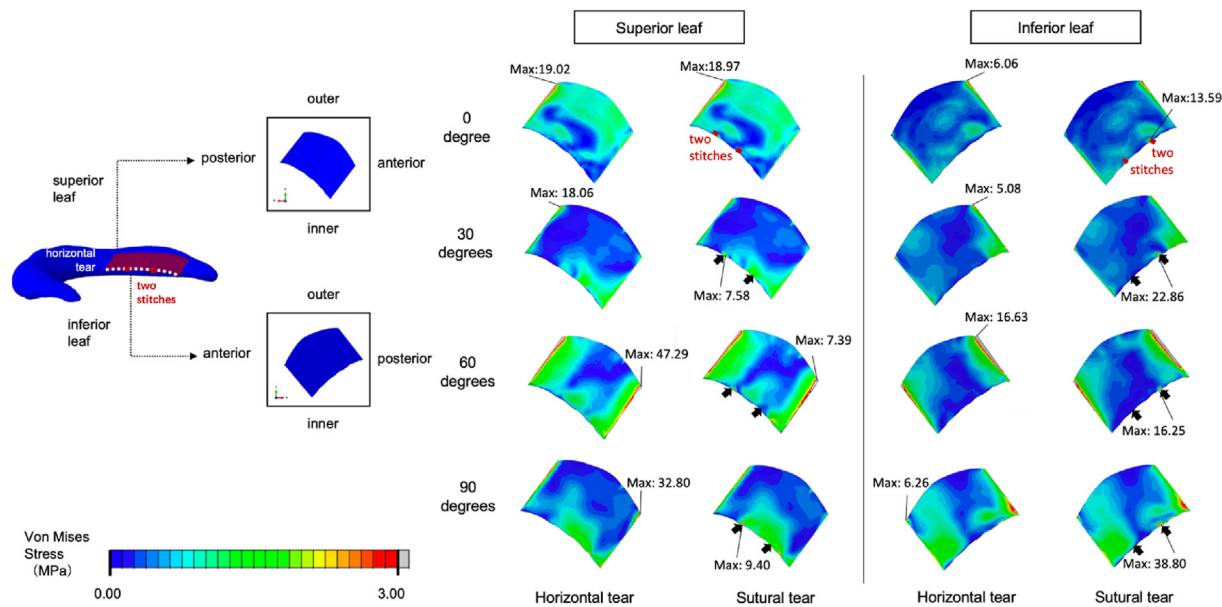


Fig. 6. Stress distribution of the superior and inferior leaflets of the tear with the knee flexion angle of 0 degree, 30 degree, 60 degree and 90 degree, around two suture stitches (arrows).

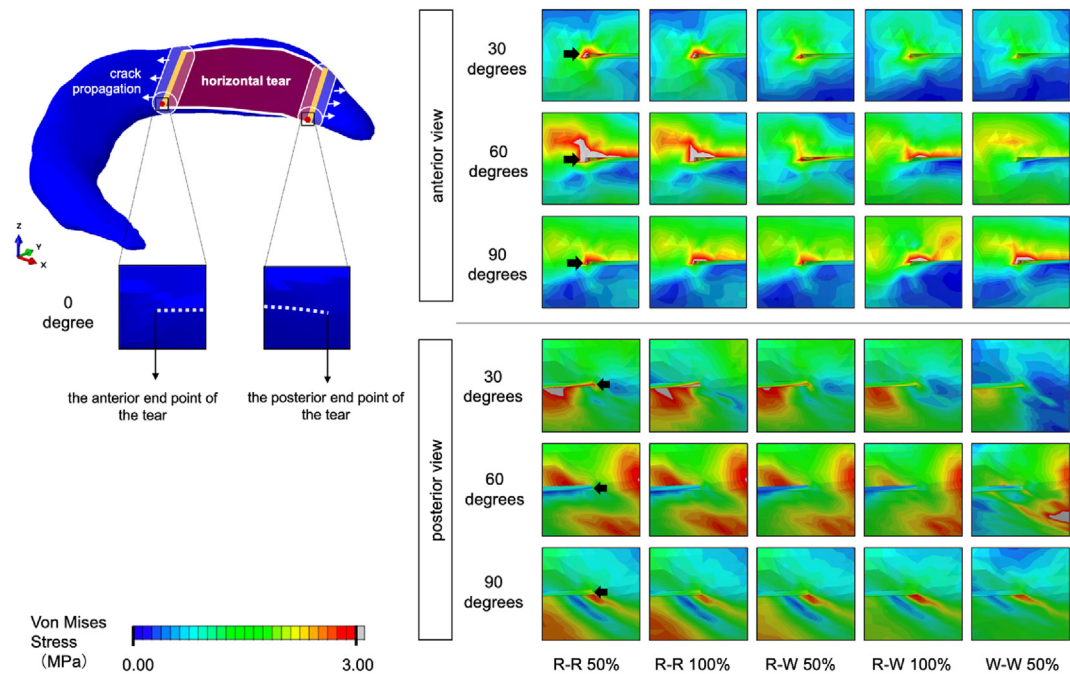


Fig. 7. During progressive healing, the stress distribution around the anterior and posterior endpoints (arrows) on the inner edge of the tear during flexion.

to simulate some typical activities by controlling the amplitude of gait input, which could provide better guidance for postoperative rehabilitation plans.

5. Conclusion

The main findings of this study indicate that after a horizontal tear of the medial meniscus, there is a notable increase in von Mises stress at the tear site, particularly at the endpoints of the tear, posing a risk of tear propagation. As the knee joint angle increases, the peak stress at the tear periphery initially rises and then decreases. Meniscal repair reduces von Mises stress within the tear region but fails to fully restore it to the undamaged state, leading to localized stress concentration near the sutured

site. After sutured repair, the peak stress of the meniscus tends to occur at the sutured site, reduces the risk of tear propagation, and mitigates stress concentration along the tear.

Ethical approval

This study was approved by the Medical Ethics Committee of Shenzhen People's Hospital (approval number: LL-KY-2023061).

CRediT authorship contribution statement

Bingtong Yan: Writing – review & editing, Writing – original draft, Visualization, Methodology, Investigation, Formal analysis, Data



curation. **Minmin Lin:** Methodology. **Yang Liu:** Resources. **Jiawei Li:** Resources, Methodology. **Linjing Peng:** Methodology. **Yifei Yao:** Methodology. **Guangheng Li:** Supervision, Conceptualization. **Chao Liu:** Writing – review & editing, Supervision, Project administration, Funding acquisition, Conceptualization.

## Declaration of competing interest

The authors declare the following financial interests/personal relationships which may be considered as potential competing interests: Chao Liu reports financial support was provided by Shenzhen Science and Technology Innovation Committee. Chao Liu reports financial support was provided by Guangdong Provincial Key Laboratory of Advanced Biomaterials. None. If there are other authors, they declare that they have no known competing financial interests or personal relationships that could have appeared to influence the work reported in this paper.

## Acknowledgments

This work was supported by Shenzhen Science and Technology Innovation Commission (Grant No. KQTD20200820113012029) and the Guangdong Provincial Key Laboratory of Advanced Biomaterials (2022B121010003).

## Appendix A. Supplementary data

Supplementary data to this article can be found online at <https://doi.org/10.1016/j.mbm.2025.100128>.

## References

- Liu T, Shen X, Ji Q, Xiao J, Zuo J. The MRI-based 3D morphologic changes of knee meniscus under knee weight-bearing and early flexion conditions. *Sci Rep*. 2021;11:22122.
- Kwon H, Brown WE, Lee CA, et al. Surgical and tissue engineering strategies for articular cartilage and meniscus repair. *Nat Rev Rheumatol*. 2019;15:550–570.
- Fox AJ, Wanivenhaus F, Burge AJ, Warren RF, Rodeo SA. The human meniscus: a review of anatomy, function, injury, and advances in treatment. *Clin Anat*. 2015;28:269–287.
- Arner JW, Ruzbarsky JJ, Vidal AF, Frank RM. Meniscus repair part 2: technical aspects, biologic augmentation, rehabilitation, and outcomes. *JAAOS-J Am Acad Orthop Surg*. 2022;30:613–619.
- Beaufils P, Pujol N. Management of traumatic meniscal tear and degenerative meniscal lesions. Save the meniscus. *J Orthop Traumatol Surg Res*. 2017;103:S237–S244.
- Brown TD, Johnston RC, Saltzman CL, Marsh JL, Buckwalter JA. Posttraumatic osteoarthritis: a first estimate of incidence, prevalence, and burden of disease. *J Orthop Trauma*. 2006;20:739–744.
- Lohmander LS, Englund PM, Dahl LL, Roos EM. The long-term consequence of anterior cruciate ligament and meniscus injuries: osteoarthritis. *Am J sports Med*. 2007;35:1756–1769.
- Lamplot JD, Tompkins WP, Friedman MV, Nguyen JT, Rai MF, Brophy RH. Radiographic and clinical evidence for osteoarthritis at medium-term follow-up after arthroscopic partial medial meniscectomy. *Cartilage*. 2021;13:588S–594S.
- Beamer BS, Walley KC, Okajima S, et al. Changes in contact area in meniscus horizontal cleavage tears subjected to repair and resection. *Arthrosc J Arthrosc Relat Surg*. 2017;33:617–624.
- Kurzweil PR, Lynch NM, Coleman S, Kearney B. Repair of horizontal meniscus tears: a systematic review. *Arthrosc J Arthrosc Relat Surg*. 2014;30:1513–1519.
- Novaretti JV, Herbst E, Chan CK, Debski RE, Musahl V. Small lateral meniscus tears propagate over time in ACL intact and deficient knees. *Knee Surg Sports Traumatol Arthrosc*. 2021;29:3068–3076.
- Arner JW, Ruzbarsky JJ, Vidal AF, Frank RM. Meniscus repair part 1: biology, function, tear morphology, and special considerations. *JAAOS-Journal Am Acad Orthop Surg*. 2022;30:e852–e858.
- Harput G, Guney-Deniz H, Nyland J, Kocabay Y. Postoperative rehabilitation and outcomes following arthroscopic isolated meniscus repairs: a systematic review. *Phys Ther Sport*. 2020;45:76–85.
- Fried JW, Manjunath AK, Hurley ET, Jazrawi LM, Strauss EJ, Campbell KA. Return-to-play and rehabilitation protocols following isolated meniscal repair—a systematic review. *Arthrosc, Sports Med Rehabil*. 2021;3:e241–e247.
- Chirichella PS, Jow S, Iacono S, Wey HE, Malanga GA. Treatment of knee meniscus pathology: rehabilitation, surgery, and orthobiologics. *PM&R*. 2019;11:292–308.
- Yin L, Chen K, Guo L, Cheng L, Wang F, Yang L. Identifying the functional flexion-extension axis of the knee: an in-vivo kinematics study. *PLoS one*. 2015;10:e0128877.
- Barber-Westin SD, Noyes FR. Clinical healing rates of meniscus repairs of tears in the central-third (red-white) zone. *Arthrosc J Arthrosc Relat Surg*. 2014;30:134–146.
- Li L, Yang L, Zhang K, Zhu L, Wang X, Jiang Q. Three-dimensional finite-element analysis of aggravating medial meniscus tears on knee osteoarthritis. *J orthop transl*. 2020;20:47–55.
- Dailey HL, Kersh ME, Collins CJ, Troy KL. Mechanical biomarkers in bone using image-based finite element analysis. *Curr Osteoporos Rep*. 2023;21:266–277.
- Yao Y, Erdemir A, Li Z-M. Finite element analysis for transverse carpal ligament tensile strain and carpal arch area. *J Biomech*. 2018;73:210–216.
- Wang J, Qi Y, Bao HRC, et al. The effects of different repair methods for a posterior root tear of the lateral meniscus on the biomechanics of the knee: a finite element analysis. *J Orthop Surg Res*. 2021;16:296.
- Zhang K, Li L, Yang L, et al. Effect of degenerative and radial tears of the meniscus and resultant meniscectomy on the knee joint: a finite element analysis. *J orthop transl*. 2019;18:20–31.
- Yang Q, Zhu X, Bao J, et al. Medial meniscus posterior root tears and partial meniscectomy significantly increase stress in the knee joint during dynamic gait. *Knee Surg Sports Traumatol Arthrosc*. 2023;31:2289–2298.
- Cheng R, Wang Z, Wang C, et al. Biomechanics of human motion. *Frontiers in Orthop Biomec*. 2020:265–300.
- Walker PS, Arno S, Bell C, Salvatore G, Borukhov I, Oh C. Function of the medial meniscus in force transmission and stability. *J Biomech*. 2015;48:1383–1388.
- Fillingham YA, Riboh JC, Erickson BJ, Bach Jr, BR, Yanke AB. Inside-out versus all-inside repair of isolated meniscal tears: an updated systematic review. *Am J Sports Med*. 2017;45:234–242.
- Vignes H, Conzatti G, Hua G, Benkirane-Jessel N. Meniscus repair: from in vitro research to patients. *Organ*. 2022;1:116–134.
- Kawamura S, Lotito K, Rodeo SA. Biomechanics and healing response of the meniscus. *Operative Tech Sports Med*. 2003;11:68–76.
- Mameri ES, Dasari SP, Fortier LM, et al. Review of meniscus anatomy and biomechanics. *Curr Rev Musculoskel med*. 2022;15:323–335.
- Norberg C, Filippone G, Andreopoulos F, et al. Viscoelastic and equilibrium shear properties of human meniscus: relationships with tissue structure and composition. *J Biomech*. 2021;120:110343.
- Danso EK, Mäkelä JTA, Tanska P, et al. Characterization of site-specific biomechanical properties of human meniscus—importance of collagen and fluid on mechanical nonlinearities. *J Biomech*. 2015;48:1499–1507.
- Zhu S, Tong G, Xiang J, et al. Microstructure analysis and reconstruction of a meniscus. *Orthop Surg*. 2021;13:306–313.
- Weber P, Woiczinski M, Steinbrück A, et al. Increase in the tibial slope in unicompartmental knee replacement: analysis of the effect on the kinematics and ligaments in a weight-bearing finite element model. *BioMed Res Int*. 2018:2018.
- Nukavarapu S, Freeman J, Laurencin C. *Regen Eng Muscoskel Tissues and Interfaces*. 2015;9:219–231.
- Jiang P, Cui J, Chen Z, Dai Z, Zhang Y, Yi G. Biomechanical study of medial meniscus after posterior horn injury: a finite element analysis. *Comput Methods Biomech Biomed Eng*. 2020;23:127–137.
- Lee J-H, Heo J-W, Lee D-H. Comparative postural stability in patients with lateral meniscus versus medial meniscus tears. *Knee*. 2018;25:256–261.
- Zhang X, Yuan S, Wang J, Liao B, Liang D. Biomechanical characteristics of tibio-femoral joint after partial medial meniscectomy in different flexion angles: a finite element analysis. *BMC Musculoskel Disord*. 2021;22:1–8.
- Chen Q, Sun F, Li Z, Taxis L, Pugno N. Nonlinear mechanics of a ring structure subjected to multi-pairs of evenly distributed equal radial forces. *Acta Mech Sin*. 2017;33:942–953.
- Risvas K, Stanev D, Benos L, Filip K, Tsaopoulos D, Moustakas K. Evaluation of anterior cruciate ligament surgical reconstruction through finite element analysis. *Sci Rep*. 2022;12:8044.
- Yang H, Ma X, Guo T. Some factors that affect the comparison between isotropic and orthotropic inhomogeneous finite element material models of femur. *Med Eng Phys*. 2010;32:553–560.
- Shepherd D, Seedhom B. The instantaneous compressive modulus of human articular cartilage in joints of the lower limb. *Rheumatol*. 1999;38:124–132.
- Daher YY, Kwon T-H, Barry M. The effect of connective tissue material uncertainties on knee joint mechanics under isolated loading conditions. *J Biomech*. 2010;43:3118–3125.
- Donahue TLH, Hull M, Rashid MM, Jacobs CR. How the stiffness of meniscal attachments and meniscal material properties affect tibio-femoral contact pressure computed using a validated finite element model of the human knee joint. *J Biomech*. 2003;36:19–34.
- Bae JY, Park KS, Seon JK, Kwak DS, Jeon I, Song EK. Biomechanical analysis of the effects of medial meniscectomy on degenerative osteoarthritis. *Med Biol Eng Comput*. 2012;50:53–60.